

Measurements in the Laminar Near-Wake of Magnetically Suspended Cones at $M_\infty = 6.3$

Isaiah M. Blankson* and Morton Finston†

Massachusetts Institute of Technology, Cambridge, Mass.

Measurements of the Pitot pressure and the recovery temperature of a cylindrical hot-film probe in the laminar near-wake of sharp, 7° half-angle, adiabatic-wall cones, at $M_\infty = 6.32$ and freestream Reynolds numbers based on model base diameter from 62,000 to 86,000 are presented. The extent of the region of measurements was from the model base to five base diameters downstream. The cones were supported with a five-degree-of-freedom magnetic model suspension system. The present study establishes several important effects of hypersonic Mach number on the structure of the axisymmetric cone near-wake when compared with the results of a previous laminar supersonic ($M_\infty = 4.3$) near-wake investigation of the same model geometry at similar Reynolds numbers. An important finding, among others, is a confirmation of the phenomenon of decreasing length of the recirculation region with increasing Mach number. Dramatic changes in the wake structure are most pronounced in the orientation and development of the lip and wake recompression shock waves. At $M_\infty = 6.32$ the viscous region was found to extend beyond the wake shock wave, whereas at the supersonic Mach number, as far back as six base diameters, there was only a gradual compressive turning of the outer inviscid flow, with the fully developed wake shock appearing farther downstream. The axial static pressure overshoot characteristics of hypersonic cone wakes was not observed in this investigation.

Nomenclature

C	= Chapman-Rubens constant = $(\rho\mu/\rho_e\mu_e)$
D, D	= cone model base diameter
H, r_B	= cone model base radius
L	= length of cone surface
M	= Mach number
p	= static pressure
P_p	= pitot pressure
Re	= Reynolds number
r	= radial coordinate measured from wake axis
T	= temperature
u	= x -component of velocity
x	= longitudinal coordinate measured from cone base
ρ	= density
χ	= hypersonic viscous interaction parameter = $\sqrt{C} M^3 / \sqrt{Re}$
μ	= viscosity coefficient
η	= Howarth coordinate defined by $\eta^2 = 2C \int_0^x \rho/\rho_e r dr$

Subscripts

l	= local value
C_L	= centerline
e	= edge of viscous region
0	= isentropic stagnation condition
m	= measured
∞	= freestream condition

Introduction

DURING the past decade a considerable amount of research, both theoretical and experimental, has been directed toward an understanding of supersonic and hypersonic wakes because of their connection with atmospheric re-

entry. Since re-entry trajectories are largely hypersonic, much of this research has been done at high Mach number. Experiments on the laminar and turbulent hypersonic cone wake have been made in ballistic ranges¹ and shock tunnels,^{2,3} thereby yielding the important gross characteristics of such flowfields in a wide Mach number and Reynolds number range.

In view of the importance of the role played by the near-wake in the development of the turbulent far-wake, recent studies have concentrated on evaluating the fluid-dynamical processes in the near-wake with the aim of providing initial profile data for far-wake computations. For two-dimensional bodies, such as wedges and cylinders, detailed wind-tunnel measurements have provided much insight into the behavior of such flowfields.⁴⁻⁶ In these cases the wakes have been almost fully laminar. In the axisymmetric case there is a scarcity of detailed wind-tunnel measurements due to the problem of model support interference. An assessment of support interference has been made by Dayman,⁷ who compared near-wakes behind wire-supported models and free-flight models. While even the smallest wires do generate some degree of interference, it appears that the fully turbulent near-wake is less susceptible to support interference than its laminar counterpart. The mean flow in the fully turbulent hypersonic axisymmetric cone-wake has been investigated, in detail, by Martellucci, et al.⁸ and Ragsdale and Darling.⁹

The application of a magnetic model suspension system completely eliminates the model support interference problem, and recently use has been made of this device in obtaining detailed flowfield measurements by McLaughlin, et al.¹⁰ in the laminar supersonic ($M_\infty = 4.3$) cone near-wake, and by Murman¹¹ in the laminar hypersonic ($M_\infty = 16$) cone-wake.

The present investigation was undertaken to provide experimental information on the flow in the fully laminar near-wake of magnetically suspended sharp, 7° half-angle, adiabatic wall cones situated in an $M_\infty = 6.32$ airstream. The key motivation for these studies was to determine for the present geometry the significant changes in the near-wake structure that are anticipated between the low supersonic Mach numbers and a Mach number of about 7, where "hypersonic freeze" is expected to occur. The present geometry was

Received June 25, 1973; revision received April 14, 1975. This research was supported by the U.S. Air Force, Office of Scientific Research, under Contract F44620-69-C-0013. Capt. Westcott H. Smith, Aeromechanics Division, OSR, served as Project Monitor.

Index category: Jets, Wakes, and Viscid-Inviscid Flow Interactions.

*Graduate Student. Currently, Associate Scientist, Research Laboratories/ITG, Xerox Corporation, Rochester, N.Y. Associate Member AIAA.

†Professor of Aeronautics and Astronautics.

chosen because detailed laminar near-wake measurements behind the same sharp-cone model at $M_\infty = 4.3$ and at similar Reynolds numbers had previously been made.¹⁰ The present experiment thus, in essence, establishes the effects of increasing Mach number on the structure of the 7° half-angle cone near-wake.

A distinguishing feature of the present flow situation, compared with the supersonic case, is that the inviscid flow about the sharp cone is characterized by the value of the hypersonic similarity parameter $M_\infty \phi_c \sim 0.8$; i.e., of order unity. It is recognized as corresponding to the nonlinear situation where the normal velocity component change across the bow shock is of the same order as the sound speed, so that the entropy gradient behind the bow shock is no longer negligible. Schematics of the two near-wake flowfields are presented in Fig. 1.

Measurements of the Pitot pressure and the recovery temperature of a cylindrical hot film probe were made in the near-wake from the cone base to five diameters downstream. The reasons for not making static pressure measurements or the hot-wire heat loss measurement are outlined in Ref. 12.

Description of Experiments

Wind-Tunnel Flow Conditions

The experiments were performed in the continuous-flow, open-jet, hypersonic wind tunnel of the MIT Aerophysics Lab. Gas Dynamics Facility using air as the test gas. The nominal $M_\infty = 6.3$ nozzle, which is operated in the slightly underexpanded condition, has a freejet cross-section area of 5.1×3.1 in.², with the usable core of inviscid fluid approximately 4.1×2.3 in.². In the experiments reported herein the freestream stagnation temperature was maintained at 470°F while the freestream stagnation pressure was varied from 61 to 90 psia. The corresponding Reynolds numbers based on model base diameter varied from 62,000 to 86,000. At these Reynolds numbers the boundary layers on the models and nozzle walls were fully laminar.

Models and Magnetic Model Suspension System

The basic model used in this investigation was a 7° half-angle, sharp-nosed cone (ratio of nose radius to base radius less than 0.01) 3 in. long with a base diameter of 0.737 in. all cones were made out of magnetic ingot iron and were approximately at the adiabatic wall temperature. For freestream Mach numbers around 6.3 the resulting ratio of sharp-cone model temperature to freestream stagnation temperature is about 0.86.

The models were supported with a five-degree-of-freedom magnetic suspension system, which has been described in detail in Ref. 13. The suspension is capable of balancing a model by means of two sets of optical systems at a predetermined position to within ± 0.005 in. and to a given angle of incidence within $\pm 0.3^\circ$, part of which is systematic error. An angle-of-attack set point range of 0° to $\pm 5\frac{1}{2}^\circ$ is available. During run conditions zero angle of attack is achieved by rotating the optical frame as a unit until the traverses of Pitot pressure (for example) appear reasonably symmetric. In this way the model angle of attack can be set to zero within $\pm 0.2^\circ$, thus essentially removing the systematic error.

Instrumentation

Measurements made in the cone near-wake consisted of the pitot pressure and the recovery temperature of a cylindrical hot-film probe. The behavior of these probes in the full Mach number and Reynolds number regimes encountered in the present measurements has been described in detail in Ref. 12.

The pitot probes were flat-ended glass tubes drawn to about 0.013 in. o.d. at the tip. Probe supports were thin, double-

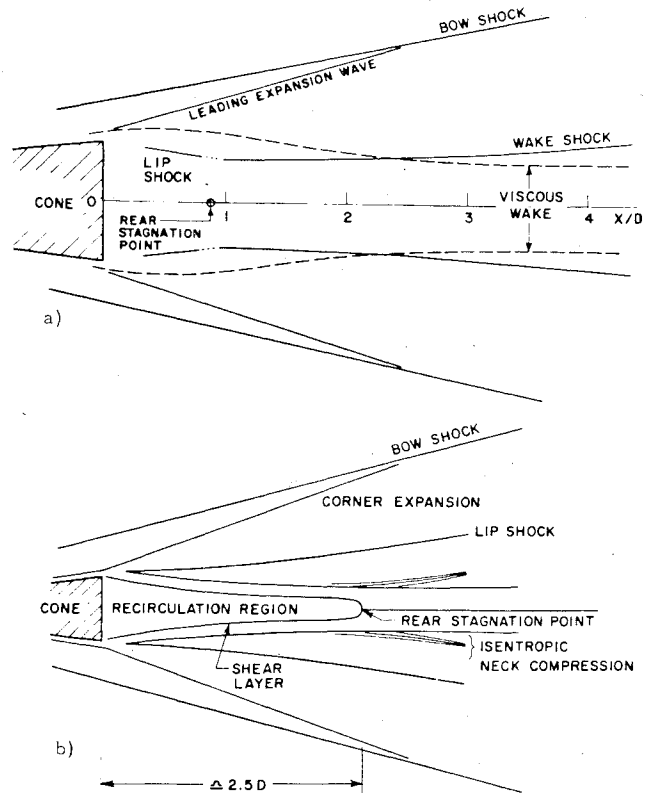


Fig. 1 a) Near-wake map at $Re_{\infty D} = 86,000$ (7° cone at $M_\infty = 6.32$); b) Near-wake map at $Re_{\infty D} = 94,000$ (7° cone at $M_\infty = 4.32$).

wedge brass stems, at the base of which was located a Statham (PA208TC) 5.0-psia pressure transducer with d.c. excitation. The transducer output was fed to the X-axis of a Moseley X-Y chart plotter on which continuous wake traverses could be recorded. The probe position signal, created by a potentiometer, was fed to the Y-axis. The pitot probe not only provides one measured quantity but also represents an accurate measurement of wake geometry. It, however, suffers from various systematic errors, of which the most severe is due to the effects of viscosity. The calibration data of Sherman¹⁴ and Matthews¹⁵ were used to obtain the viscous corrections to the pitot pressure measurements. Details of these procedures are presented in Ref. 12. Two geometrically similar pitot probes of different sizes were used for the measurements. No variations in the measured pitot pressure could be detected in the results. The pitot probes were also shown by calibration to be virtually insensitive to angulation in a $\pm 20^\circ$ range.

Total temperature measurements were deduced from the measured recovery temperature of a cylindrical hot-film probe (Thermal Systems, Inc., Probe 1276-10). The advantages of the hot film are twofold. Firstly, it can be made an order of magnitude larger than the hot wire without sacrificing its sensitivity, so that deviations from the continuum regime are small. Secondly, the end-loss correction, which must be incorporated when a hot wire is used, is almost completely eliminated. In this ideal situation the heat-transfer characteristics of an infinite wire are implied and use can be made of the recovery factor curve for an infinite wire¹⁶ to get the local total temperature from the measured recovery temperature. The results of calibrations in known flowfields are presented in Ref. 12. In these measurements a constant current of 0.753 mamp (furnished by a Shapiro-Edwards Model 50A) was driven through the hot film and the d.c. amplified output was fed to a Moseley X-Y chart plotter.

Both pitot and hot-film probes were supported in a probe drive capable of motion in three orthogonal directions. Measurements were made by continuously traversing the

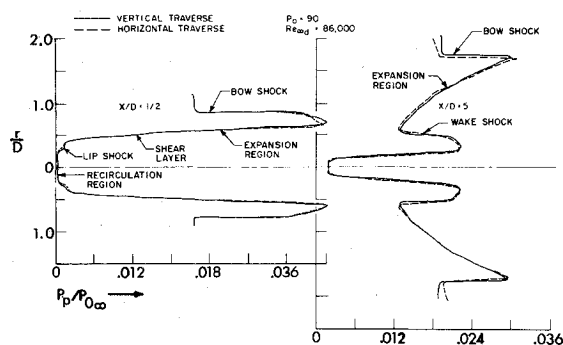


Fig. 2 Comparison of horizontal and vertical traverses.

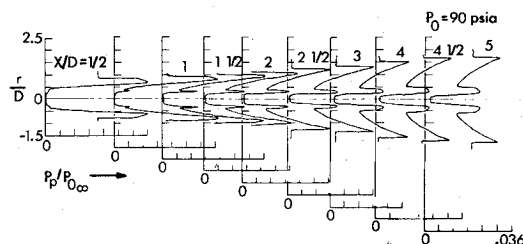


Fig. 3 Pitot pressure profiles at zero angle of attack (sharp cone). $Re_{\infty} = 86,000$.

probe vertically (y -axis) or horizontally (z -axis) through the axis of symmetry (x -axis) of the model, each traverse extending about $\pm 2.0D$ from the model axis. An indication of flowfield symmetry is obtained by comparing the horizontal and vertical traverses at each axial location.

Data Reduction Procedures

Three known independent parameters are necessary for a unique and complete reduction of the raw data to the primary flowfield variables. In the present investigation the hot-film recovery temperature, and the pitot pressure measurements were used to divide the near-wake into an outer inviscid wake and an inner viscous core. In the inviscid region the three independent parameters are the measured pitot pressure, the measured recovery temperature, and the stagnation pressure behind the bow shock determined from its slope. In the viscous region the pitot pressure and recovery temperature measurements are supplemented with the assumption that at each axial location the static pressure may be taken as approximately constant from the wake axis to the edge of the high shear region.

Static pressure measurements presented in Ref. 10 showed that the radial static pressure variation from the axis to the edge of the viscous region is negligible both in the recirculation region and downstream in the inner wake. It must be noted that this assumption allows for axial static pressure gradients. Upstream of $X/D = 2\frac{1}{4}$, where the wake recompression shock is embedded in the viscous core, the static pressure jumps across the wake shock wave are deduced from the corresponding pitot pressure jumps. Details of these procedures are summarized in Ref. 12.

Experimental Results and Discussion

Pitot Pressure Measurements and Location of Rear Stagnation Point

The results of the pitot pressure measurements in the range $62,000 < Re_{\infty} < 86,000$ are presented in Ref. 12. The pitot pressure measurements corresponding to $Re_{\infty} = 86,000$ are presented in Figs. 2 and 3. At each axial location continuous traverses of pitot pressure were recorded in two orthogonal

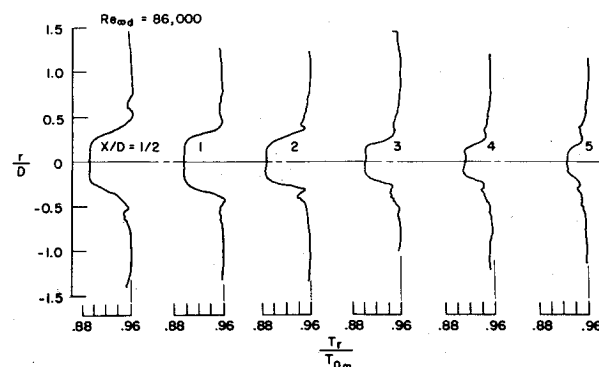


Fig. 4 Hot-film recovery temperature in sharp cone wake $M_{\infty} = 6.3$.

directions. An example of wake symmetry at zero angle of attack is shown in Fig. 2. Here both traverses are radial; one is vertical and the other is horizontal. Besides providing one measured quantity the pitot profile represents an accurate measurement of wake geometry. In Fig. 2 various flowfield features may be identified. Noticeable features are the bow shock wave, the wake recompression shock wave, and also the decrease of pitot pressure across the expansion wave system. A lip shock wave, which may be identified in the profile at $X/D = \frac{1}{2}$, is much weaker than the wake shock wave. Also in this profile between the location of the leading expansion wave and the bow shock wave the pitot pressure exhibits the gradual monotonic decrease, which is characteristic of conical irrotational flow. The edge of the viscous core is easily detected in the pitot pressure profile at $X/D = 5$. In the profile at $X/D = \frac{1}{2}$, however, the pitot pressure gradients in the inviscid region are of the same order as those of the shear layer. In such cases the corresponding hot-film recovery temperature profile was used to define the wake edge.¹²

The overall development and geometry of the near-wake is presented by the pitot profiles in Fig. 3. The bow shock angle, as determined from these measurements, was virtually constant at $12^{\circ} \pm 1^{\circ}$. Examination of the pitot profiles reveals that the leading expansion wave does not intersect the bow shock until about $X/D = 2\frac{1}{2}$. The development of the wake shock wave is not only rapid but rather distinctive. The wake shock originates in the vicinity of $X/D = 0.8$ and emerges from the viscous core at $X/D = 2\frac{1}{4}$.

The present experiments, in essence, portray the changes that occur in the 7° half-angle cone near-wake structure due to the sole variation of freestream Mach number from $M_{\infty} = 4.32$ to $M_{\infty} = 6.32$. The various changes in the near-wake structure are summarized in Figs. 1a and 1b. An important difference concerns the orientation of the lip shock wave in relation to the wake shock wave. At $M_{\infty} = 4.32$ the two shocks are clearly distinguishable from each other. The lip shock does not intersect the wave shock until far downstream, and between the model base and about six diameters downstream there is only a smooth, compressive turning of the outer inviscid flow back to the freestream direction. The fully developed wake shock, which is formed by the coalescence of the compression waves, is formed farther downstream. At $M_{\infty} = 6.32$, however, the lip shock and the wave recompression shock, as determined from the pitot pressure surveys, appear to merge and form a continuous shock structure. A similar result was also found by Hama¹⁷ in his supersonic wedge experiments. It occurs because the lip shock turns more and more towards the wake axis with increasing Mach number until it eventually coalesces with the wake shock. Another striking difference is the transverse extent of the viscous region in relation to the lip shock and wave shock locations. The $M_{\infty} = 4.32$ results indicate that the viscous core is contained within the wake shock boundaries, whereas at $M_{\infty} = 6.32$ the viscous region extends beyond the wake shock location, indicating that viscous effects would be important

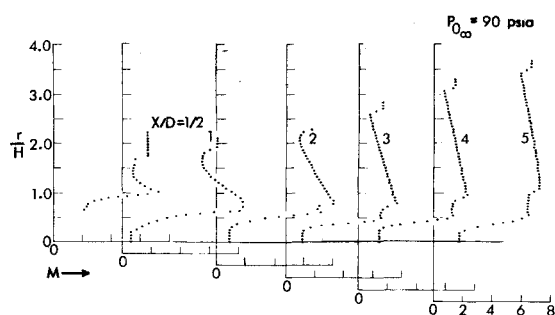


Fig. 5 Calculated Mach number profiles for $Re_{\infty D} = 86,000$.

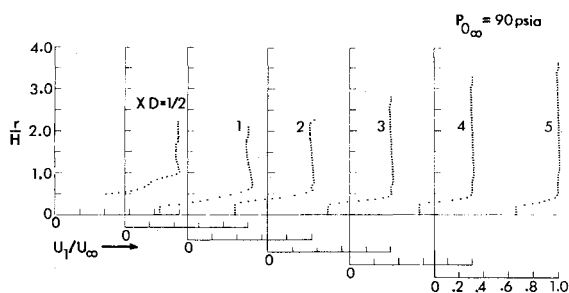


Fig. 6 Calculated velocity profiles for $Re_{\infty D} = 86,000$.

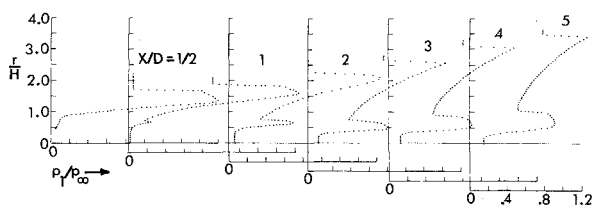


Fig. 7 Calculated density profiles for $Re_{\infty D} = 86,000$.

outside the wake shock wave. Examination of pitot pressure surveys of $M_{\infty} = 4.32^{10}$ shows a region of constant pitot pressure between the lip shock and the edge of the shear layer. This behavior is absent in the present measurements. This indicates that the large region of rotational inviscid flow, resulting from the wide divergence of streamlines originally contained in the body boundary layer, and so prominent in hypersonic wakes, is absent at the supersonic Mach number.

The rear stagnation point location is in the vicinity of $X/D = 1$ (Fig. 1a). This is in good agreement with the summary curve of Martellucci, et al.,⁸ which shows the variation of the rear stagnation point location with trailing edge Reynolds number. The data used by Martellucci, et al. comprise measurements from not only cones but also wedges and cylinders under cold-wall and adiabatic-wall temperatures and even both laminar- and turbulent-flow conditions. They find that for $M_{\infty} > 5$ the rear stagnation points for all cases are around 0.8 base diameters (heights) downstream of the cone base. For cones, the variation of the rear stagnation point location with Mach number for Mach numbers between the low supersonic values and about 5 was, however, not considered. The measured location of the rear stagnation point at $M_{\infty} = 4.32^{10}$ was placed at about $2\frac{1}{2}$ diam downstream of the cone base. These results are confirmed from Schlieren photographs of the 7° half-angle cone near-wake at $M_{\infty} = 4.32$ and $M_{\infty} = 6.32$. The longer recirculation region appears to be characteristic of the laminar supersonic cone near-wake, as is also evidenced by the supersonic Mach number, free-flight cone-wake Schlieren results of Dayman¹⁸ and King.¹⁹ The important result here is that this investigation has confirmed the phenomenon of decreasing length of the recirculation region with increasing Mach number.

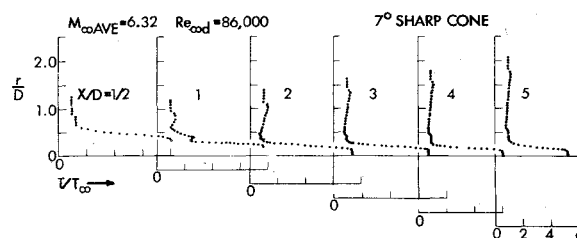


Fig. 8 Calculated static temperature profiles for $Re_{\infty D} = 86,000$.

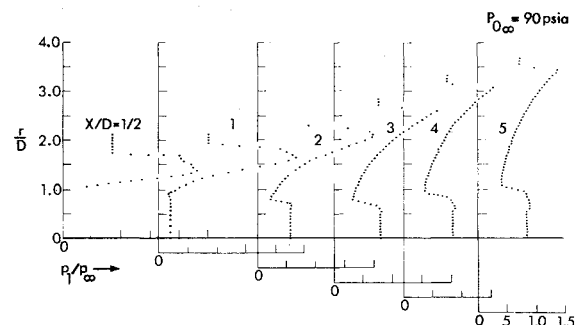


Fig. 9 Calculated static pressure profiles for $Re_{\infty D} = 86,000$.

Total Temperature Measurements and Computed Results

The raw hot-film recovery temperature measurements for $Re_{\infty D} = 86,000$ are presented in Fig. 4. These measurements display the shear layer total temperature overshoots that are typical of adiabatic-wall boundary layers. In addition to providing one measured quantity, the hot-film recovery temperature measurements enable the determination of the wake edge. The wake edge determined in this fashion corresponds to the boundary between that portion of the flow unaffected by the temperature of the wall and that portion which has been affected by the wall through the action of viscosity and heat conductivity. Downstream of $X/D = 2\frac{1}{2}$ the wake edge may also be deduced from the pitot pressure measurements. In these regions the wake edge defined from the hot-film measurement was coincident with that defined by the pitot profile.

Calculated wake flow properties corresponding to $Re_{\infty D} = 86,000$ are presented in Figs. 5-9. These results are also conveniently summarized in the distribution of axial-flow variables presented in Fig. 10. The calculated Mach number distributions (Fig. 5) reveal the slow decay of the Mach number defect across the wake, indicating a fully laminar behavior. The calculated velocity (Fig. 6) and density (Fig. 7) distributions indicate that extremely low densities are present in the immediate vicinity of the wake axis. The mass flow in the viscous core is seen to be a rather small fraction of the total mass flow in the near-wake. The calculated temperature distributions (Fig. 8) show that the peak temperatures in the adiabatic-wall cone near-wake occur along the wake axis. The momentum defect and the temperature excess will persist for many base diameters downstream. The calculated static pressure distributions are presented in Fig. 9. Along the wake axis the static pressure rises monotonically towards its freestream magnitude from below. The distribution of axial static pressure is one of the elements that is used to characterize near-wakes. Planar-wakes generally show a monotonic rise in pressure from the base to the freestream value. For cone-wakes, especially at the higher Mach numbers, some investigations have revealed pressure overshoots in the neck region, followed by a decay towards P_{∞} from above. This behavior is attributed to the implosion of streamlines in the inner portion of the outer inviscid rotational flow.²⁰ In the work of Finson and Weiss²⁰ a theoretical result is the prediction of a pressure overshoot in the recompression region,

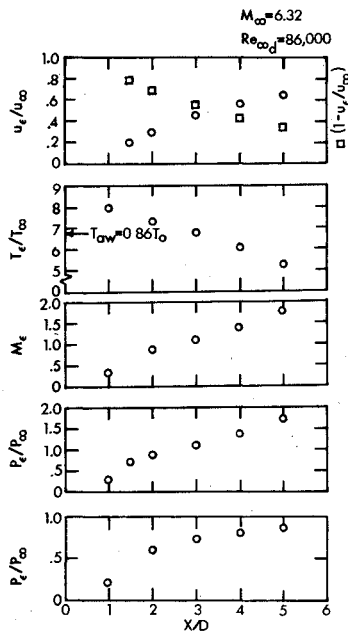


Fig. 10 Axial distribution of wake flow variables.

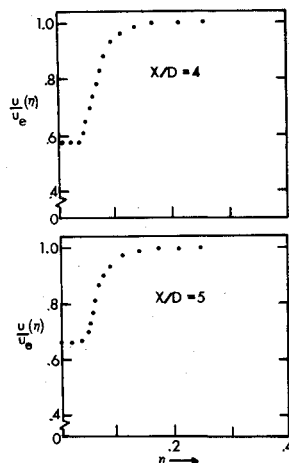


Fig. 11 Velocity profiles in Howarth coordinates.

which scales like $\chi \ln M_e / \chi$. This is, in fact, confirmed experimentally by Murman¹¹ among others, but was not observed in the present investigation. For $Re_{\infty D} = 86,000$, the scaling parameter $\chi \ln M_e / \chi$ has the value 0.95, for which the theory predicts no overshoot. The present experiments thus provide an important confirmation of the theory of Finson and Weiss.²⁰

On comparing the present measurements ($M_\infty = 6.3$) with those of Murman ($M_\infty = 16.35$), it is seen that the two appear very similar in both flowfield mapping and pitot pressure measurements. Overlays of corresponding pitot pressure profiles¹² indicate that the major differences are the absence of a lip shock and the existence of a pressure overshoot in Murman's investigation, and also his obviously stronger bow shock.

In Fig. 11 is presented the calculated velocity profiles at $X/D = 4$ and $X/D = 5$ in terms of η , the Dorodnitsyn-Howarth density contracted coordinate. The relative density change across the viscous wake is evidenced in a comparison between Figs. 6 and 11. These velocity profiles have also not yet developed into gaussians, the latter being a mathematical convenience that has been used (as initial profiles, for example) in the work of Finson and Weiss.²⁰

Conclusions

Measurements of the pitot pressure and the recovery temperature of a cylindrical hot-film probe have been made in the near-wake region of sharp and spherically blunted 7° half-angle cones from the model base to five base diameters downstream. The cones were magnetically suspended in an $M_\infty = 6.32$ continuous-flow wind tunnel and were approximately at the recovery temperature. The majority of the measurements were performed at a freestream Reynolds number $Re_{\infty D} = 86,000$. A simplified data reduction scheme, which combines the above measurements with assumptions on static pressure, is shown to be useful and reliable. The near-wake flowfield is mapped with the exception of the region interior to the recirculating bubble.

Several important effects of hypersonic Mach number are established by the present investigation when compared with a previous supersonic ($M_\infty = 4.32$) laminar near-wake study, which employed the same model geometry at identical freestream Reynolds numbers. The phenomenon of decreasing length of the recirculation region with increasing Mach number is clarified by the present investigation. The shorter recirculation region observed here is typical of hypersonic near-wakes, while the length of the recirculation region is significantly longer at the lower Mach numbers. The axial static pressure overshoots so prominent in hypersonic-cone near-wakes were not observed in the present measurements. Dramatic changes in the wake structure are most pronounced in the orientation and development of the lip and wake recompression shocks, and also in the radial extent of the viscous region. The effect of hypersonic Mach number is seen to generate a near-wake flowfield whose structure is considerably more complicated than that found at $M_\infty = 4.32$, since now the viscous region extends beyond the wake shock wave, indicating that viscous effects would be important outside the wake shock.

References

- ¹Pallone, A. J., Erdos, J. I., and Eckerman, J., "Hypersonic Laminar Wakes and Transition Studies," *AIAA Journal*, Vol. 2, May 1964, pp. 855-963.
- ²Cresci, R. J. and Zakkay, V., "An Experimental Investigation of the Near Wake of a Slender Cone at $M_\infty = 8$ and 12," *AIAA Journal*, Vol. 4, Jan. 1966, pp. 41-46.
- ³Todisco, A. and Pallone, A. J., "Near Wake Flow-Field Measurements," *AIAA Journal*, Vol. 3, Nov. 1965, pp. 2075-2080.
- ⁴Dewey, C. F., Jr., "Near-Wake of a Blunt Body at Hypersonic Speeds," *AIAA Journal*, Vol. 3, June 1965, pp. 1001-1010.
- ⁵Batt, R. G. and Kubota, T., "Experimental Investigation of Laminar Near-Wakes Behind 20° Wedges at $M_\infty = 6$," *AIAA Journal*, Vol. 6, Nov. 1968, pp. 2077-2083; see also *AIAA Journal*, Vol. 7, 1969, pp. 2064-2071.
- ⁶Behrens, W., "The Far Wake Behind Cylinders at Hypersonic Speeds, Pt. 1: Flow Field," *AIAA Journal*, Vol. 5, Dec. 1967, pp. 2135-2141.
- ⁷Dayman, B., Jr., "Support Interference Effects on the Supersonic Wake," *AIAA Journal*, Vol. 1, Aug. 1963, pp. 1921-1923.
- ⁸Martellucci, A., Trucco, H., and Agone, A., "Measurements of the Turbulent Near Wake of a Cone at Mach 6," *AIAA Journal*, Vol. 4, March 1966, pp. 385-391.
- ⁹Ragsdale, W. C. and Darling, J. A., "An Experimental Investigation of the Turbulent Wake Behind a Cone at Mach 5," TR 66-95, 1966, Naval Ordnance Lab., White Oak, Md.
- ¹⁰McLaughlin, D. K., Carter, J. E., Finston, M., and Forney, A. J., "Experimental Investigation of the Mean Flow of a Laminar Supersonic Cone-Wake," *AIAA Journal*, Vol. 9, March 1971, pp. 479-484.
- ¹¹Murman, E. M., "Experimental Studies of a Laminar Hypersonic Cone Near Wake," *AIAA Journal*, Vol. 7, Sept. 1969, pp. 1724-1730.
- ¹²Blankson, I. M., "Experimental Investigation of a Laminar Axisymmetric Cone Near-Wake at $M_\infty = 6.3$," Ph.D. thesis, June 1973, Dept. of Aeronautics and Astronautics, MIT, Cambridge, Mass.

¹³Tilton, E. L., Parkin, W. J., Covert, E. E., Coffin, J. B., and Chrisinger, J. E., "The Design and Initial Operation of a Magnetic Model Suspension and Force Measurement System," *Journal of the Royal Aeronautical Society*, Vol. 67, Nov. 1963, pp. 717-744.

¹⁴Sherman, F. S., "New Experiments on Impact Pressure Interpretation in Supersonic and Subsonic Rarefield Air Streams," NACA TN 2995, 1953.

¹⁵Matthews, M. L., "An Experimental Investigation of Viscous Effects on Static and Impact Pressure Probes in Hypersonic Flow," Memo 44, June 1958, GALCIT, Hypersonic Research Project, Pasadena, Calif.

¹⁶Dewey, C. F., Jr., "A Correlation of Convective Heat-Transfer and Recovery Temperature Data for Cylinders in Compressible

flow," *International Journal of Heat and Mass Transfer*, Vol. 8, 1965, pp. 245-252.

¹⁷Hama, F. R., "Experimental Studies on the Lip Shock," AIAA Paper 67-29, New York, N.Y., 1967.

¹⁸Dayman, B., Jr., "Free-Flight Testing in High-Speed Wind Tunnels," NATO, AGARD 113, 1966.

¹⁹King, H. H., "Some Base Flow Closure Angle Results in Free Flight," *Electro-Optical Systems*, Research Note 21, 1964, Pasadena, Calif.

²⁰Finson, M. L. and R. F. Weiss, "Theoretical Investigation of the Hypersonic Axisymmetric Near-Wake Recompression Region," AVCO Everett Research Rept. 334, July 1969, Everett, Mass.

From the AIAA Progress in Astronautics and Aeronautics Series . . .

HYPERSONIC FLOW RESEARCH—v. 7

Edited by Frederick R. Riddell, Avco Corporation

Hypersonic gasdynamics is the principal concern of the twenty-two papers in this volume, encompassing flow at low Reynolds numbers, chemical kinetic effects in hypersonic flow, and experimental techniques.

Papers concerned with flow at low Reynolds numbers treat boundary layer and stagnation phenomena in a number of situations, including flow about reentry bodies, nonequilibrium boundary layer flow, and bodies in atmospheric transition. Chemical kinetics papers concern high temperature air, reactions about axisymmetric hypersonic vehicles, wakes, optical radiation, and radiative heating at reentry speeds.

Surface pressure and heat transfer are predicted for lifting reentry vehicles. Conical flow equations are solved for reentry vehicles, and entropy layer properties of such vehicles are related to nose bluntness.

Hotshot, gun-type, and hypersonic arc tunnels are all evaluated for heat transfer experiments and gasdynamic experiments, citing calibration, comparative results, convenience, and economy. A free-flight range is evaluated and tested, and future prospects for all types of hypersonic test facilities are described.

758 pp., 6 x 9, illus. \$19.00 Mem. & List

TO ORDER WRITE: Publications Dept., AIAA, 1290 Avenue of the Americas, New York, N. Y. 10019